



Accepted Article

Title: Fine-Tuning Ligand Field with Schiff Base Ligand in Dy²⁺ Compounds

Authors: Sanping Chen

This manuscript has been accepted after peer review and the authors have elected to post their Accepted Article online prior to editing, proofing, and formal publication of the final Version of Record (VoR). This work is currently citable by using the Digital Object Identifier (DOI) given below. The VoR will be published online in Early View as soon as possible and may be different to this Accepted Article as a result of editing. Readers should obtain the VoR from the journal website shown below when it is published to ensure accuracy of information. The authors are responsible for the content of this Accepted Article.

To be cited as: Eur. J. Inorg. Chem. 10.1002/ejic.201601188

Link to VoR: <http://dx.doi.org/10.1002/ejic.201601188>

Fine-Tuning Ligand Field with Schiff Base Ligand in Dy₂ Compounds

Min Li⁺,^[a] Haipeng Wu⁺,^[a] Sheng Zhang⁺,^[a, b] Lin Sun,^[a] Hongshan Ke,^[a] Qing Wei,^{*[a]} Gang Xie,^[a] Sanping Chen,^{*[a]} Shengli Gao^[a]

^[a] M. Li,⁺ H. Wu,⁺ Dr. S. Zhang,⁺ L. Sun, Dr. H. Ke, Prof. Q. Wei, G. Xie, Prof. S. Chen, Prof. S. Gao

Key Laboratory of Synthetic and Natural Functional Molecule Chemistry of Ministry of Education

College of Chemistry and Materials Science

Northwest University

Xi'an 710069, China

E-mail: sanpingchen@126.com

weiqg@126.com

<http://chem.nwu.edu.cn/teacher.php?id=74>

^[b] Dr. S. Zhang⁺

College of Chemistry and Chemical Engineering

Baoji University of Arts and Sciences

Baoji 721013, China

^[*] These authors have equal contribution to this work.

***Corresponding author**

Prof. Sanping Chen

E-mail: sanpingchen@126.com

Abstract

Three dinuclear coordination compounds, $[\text{Ln}_2(\text{Hhms})_2(\text{NO}_3)_4] \cdot \text{MeCN}$ ($\text{Ln} = \text{Dy}$ (**1**) and Er (**2**)) and $[\text{Dy}_2(\text{Hhms})_2(\text{NO}_3)_2(\text{H}_2\text{O})_3] \cdot (\text{NO}_3)_2 \cdot \text{MeCN} \cdot (\text{H}_2\text{O})_2$ (**3**), were isolated with asymmetric schiff base ligand 1-(2-hydroxy-3-methoxybenzylidene)-semicarbazide (H_2hms). The potentially tetradentate ONOO donor of the ligand has revealed considerable metal ion selective phenoxo bridging in **1-3**. Compounds **1** and **2** display the hula-hoop-like coordination geometry, whereas such geometry is broken by an additional $\mu_2\text{-OH}_2$ bridge in compound **3**. The structural discrepancies induced by the different bridge manners in **1** and **3** affect the magnetism. Compound **1** exhibits slow relaxation of the magnetization, suggesting single-molecule magnet (SMM) behavior, while no out-of-phase alternating-current signal can be observed in **3**. Meanwhile, compared with a reported Dy_2 compound, **1** occupies the same coordination group but shows different magnetic properties attributing to the different ligand backbone. Fine-tuning of ligand field is dominated by conjugated degree of ligand backbone that cause the SMM/non-SMM behavior.

Introduction

With 4f-electrons featuring inherently large unquenched orbital angular momentum, lanthanide-based single molecule magnets (SMMs) have been a promising candidate for realizing the potential applications in high density information storage, quantum computing and molecular spintronics devices.^[1] SMMs display slow relaxation of the magnetization of purely molecular origin, while increased SMMs performance with greater relaxation energy barriers (U_{eff}) and blocking temperature (T_{B}) are long-term aspirations for researchers in the field of SMMs.^[2] Under the unswerving efforts, mononuclear systems have rapidly developed and many decisive influencing factors contributing to the magnetic properties have been confirmed through theoretical and experimental studies. Recently, a series of mononuclear dysprosium coordination compounds with high performance magnetic relaxation behavior were reported by the M. Tong, S.

Gao and J. Tang groups, respectively.^[3] The results indicate that the local symmetry or charge distributional symmetry around the dysprosium ion can efficiently suppress the quantum tunnelling of magnetization and stabilize the largest $\pm m_J$ state. Furthermore, a strong axial and weak equatorial ligand field bring about a high axiality in the low-lying Kramers doublets facilitating magnetic relaxation climbing up to a higher excited state energy levels. The significant relaxation mechanism investigation offers a practical way to design highly efficient mononuclear SMMs. However, a comprehensive research has been rarely explored in polynuclear lanthanide (Ln^{III}) SMMs due to increasing Ln^{III} centers bring much more non-negligible complexity of the structure.^[4] Thus, it is necessary to acquire a deeper understanding for the mechanism and source of SMMs in multinuclear Ln^{III} coordination compounds so that provide better guidance for the design of new SMMs.^[5] Therein, dinuclear Ln^{III} SMMs systems are supposed as representative to have a better understanding on the magneto-structural correlation.^[6] Indeed, some research based on dinuclear SMM behavior have been reported. Muralee *et al.* investigated a series of dinuclear Ln^{III} coordination compounds whose energy barrier have been improved due to highly electron-withdrawing substitutes on the terminal ligands.^[7] Additionally, Long *et al.* successfully constructed strong magnetically coupled Tb^{III} coordination compound featuring a N_2^{3-} radical bridge, giving rise to a high T_B of 14 K.^[8] These outstanding contributions suggest that either a small alteration in ligand systems or magnetic interaction between metal sites can produce changes in magnetic behavior.

It is noted that organic ligands play a vital role in the synthesis of discrete SMMs as well as modulation of SMMs properties.^[9] Schiff base ligand possessing rich O, N-based multi-chelating sites have been widely used in the synthesis of many lanthanide-based coordination compounds.^[10] Therein, the ligand systems formed by reaction between the o-vanillin and acylhydrazine derivatives is a particularly good choice due to the phenoxo atoms of the o-vanillin can be deprotonated to act as a bridge between metal ions, producing a super-exchange pathway.^[11] Besides, the modification of acylhydrazine derivatives terminal group offers a series of slightly varied ligand systems to study the ligand field effects on SMMs properties of Ln^{III} coordination compounds.

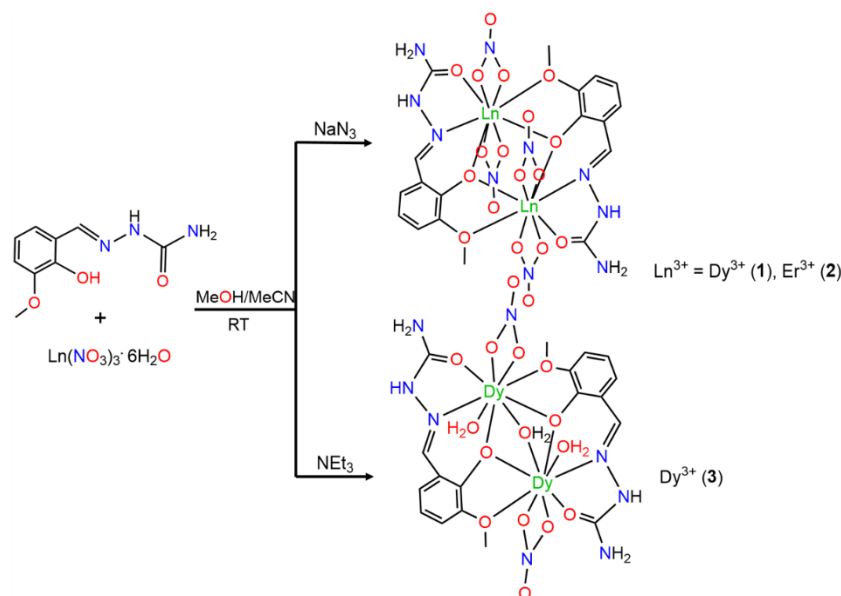
Therefore, in order to have a better understanding for SMM behavior of dinuclear systems, potentially tetradentate phenoxo-bridged schiff base ligand

(2-hydroxy-3-methoxybenzylidene)-semicarbazide (H_2hms) was chosen to assemble Ln_2 coordination compounds. As a result, three salen-type coordination compounds, $[Ln_2(Hhms)_2(NO_3)_4] \cdot MeCN$ ($Ln = Dy$ (**1**) and Er (**2**)), and $[Dy_2(Hhms)_2(NO_3)_2(H_2O)_3] \cdot (NO_3)_2 \cdot MeCN \cdot (H_2O)_2$ (**3**), have been isolated. Crystal structures, magnetic properties and luminescence of three coordination compounds have been investigated. Besides, we contrastively discussed the SMM/non-SMM behavior of two groups of Dy_2 compounds: **1** and **3**; **1** and a reported coordination compound $[Dy_2(Hhmc)_2(NO_3)_4] \cdot THF \cdot MeCN$ by Lin group.^[12] Therein, reported $[Dy_2(Hhmc)_2(NO_3)_4] \cdot THF \cdot MeCN$ occupies the same coordination group but differs on ligand backbone with **1**. The occurrence of SMM behavior was realized via changing conjugated degree of ligands. Electronic modifications in the ligand backbone while maintaining the coordination group of the metal centers provides an elegant model to explore the influence of ligand field effects on SMM properties.^[7, 13] To the best of our knowledge, most of reported dinuclear coordination compounds studies were based on the replacement of the terminal β -diketonate ligands,^[6b, 7, 14] but fine-tuning ligand field through schiff base ligand are relatively rare.^[15]

Results and discussion

Synthetic Aspects

The hydrazone ligand, (2-hydroxy-3-methoxybenzylidene)-semicarbazide (H_2hms) possesses multiple coordination sites (namely, a methoxy group, a phenolic oxygen, an imine nitrogen, and carbonyl oxygen) which are suitable for binding to lanthanide metal ions. In addition, hydrated lanthanum nitrates were treated with different bases (sodium azide or triethylamine) in the presence of the ligand to generate two types of lanthanide compounds with different bridge manners (Scheme 1). The different structure of compounds indicate that the reaction is sensitive to the selection of base, and changing bridge manner between metal ions is crucial to magnetic properties. Similar works have been mentioned that Tang and co-workers have prepared base-assisted lanthanide compounds with different bridging-modes.^[16] Therefore, through tuning bases, understanding and elucidating the self-assembly mechanism in solution systems for construction of Dy^{III} -based SMMs is necessary.



Scheme 1. Synthesis scheme of dinuclear lanthanide compounds **1-3**.

Structural description

$[\text{Ln}_2(\text{Hhms})_2(\text{NO}_3)_4] \cdot \text{MeCN}$ ($\text{Ln} = \text{Dy}$ (1) and Er (2))

Single-crystal X-ray analysis reveals that coordination compounds **1** and **2** are isomorphous dinuclear coordination compounds in the space group $P\bar{1}$. As a representative, only the structure of compound **1** is discussed in detail. Compound **1** is centrosymmetric and each Dy^{III} ion is nine-coordinated with a monocapped square antiprism geometry (Figure S1(a)). The geometry of **1** was calculated with the SHAPE 2.1 software (Table S1).^[17] The coordination spheres of Dy^{III} are completed by the pentagonal plane which is composed of O1, O2, O2A, O3A and N1A from two antiparallel Hhms⁻ ligands and interpenetrating tetrahedral arrangement which is composed of O5, O7, O8 and O9 from two nitrate anions (bidentate) (Figure 1). The dimeric Dy1 and Dy1A are bridged by two deprotonated phenoxyl oxygen atoms (O2 and O2A) of the ligands, giving rise to a four-membered $\text{Dy}_2(\mu_2\text{-O})_2$ core with Dy-O bond lengths of 2.290(2) and 2.364(2) Å, the Dy1...Dy1A distance being 3.6685(3) Å and two the Dy1-O-Dy1A angles of 103.877(15) $^\circ$. The nine-coordinate Dy^{III} center exhibits what has been described as a hula-hoop-like geometry, where the cyclic ring (hula hoop) is defined by the atoms O1, O2, O2A, O3A and N1A.

The packing arrangement of coordination compound **1** shows weak intermolecular N-H...O

interactions involving nitrogen atoms of the primary amine and secondary amine part of Hhms^- and two opposite coordinated nitrate oxygen atoms. The smallest $\text{Dy}_2 \cdots \text{Dy}_2$ separation is longer than 7.5 Å. The packing of adjacent Dy_2 molecules generate 2D layers, extending along the ab plane (Figure S2).

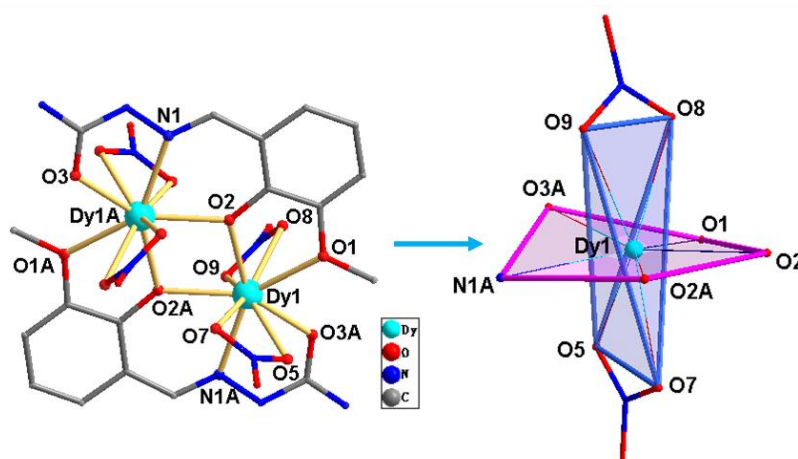
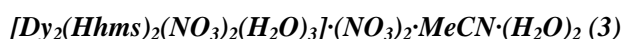


Figure 1. Molecular structures of coordination compound **1** (left) and core structural representation of **1** (right).

Hydrogen atoms and lattice solvent molecules are omitted for clarity. (A: $-x + 1, -y + 1, -z + 1$).



The single-crystal X-ray structure of the coordination compound **3** is depicted in Figure 2. Compared with compound **1**, each Dy^{III} centers are also coordinated with pentagonal plane (O1, O2, O5, O6 and N4 for Dy1, O2-O5 and N1 for Dy2) from two antiparallel Hhms^- ligands, but the remaining sites of each Dy^{III} ions are completed with one nitrate molecule (bidentate) (O13, O14 for Dy1, O10, O11 for Dy2), one water molecule (O8 for Dy1, O9 for Dy2) and an additional $\mu_2\text{-OH}_2$ (O7) bridge. Dy1 and Dy2 are bridged by a $\text{Dy}_2(\mu\text{-O})_3$ core, which is created by two phenoxides of the Hhms^- ligands (O2 and O5) and one water oxygen bridge (O7) with a $\text{Dy1} \cdots \text{Dy2}$ distance of 3.6685(3) Å and three Dy-O-Dy bond angles of 101.074(16)°, 89.823(13)° and 100.681(15)°. As for **1**, the geometry was determined by the SHAPE 2.1 software for **2**.^[17] The deviation from ideal C_{4v} symmetry was recorded by a CSM of 1.151 for Dy1 and 1.102 for Dy2, indicating much smaller deviations from the capped square antiprismatic polyhedron than compound **1** (Table S2). The coordination polyhedron of Dy ions for **2** is revealed in Figure

S1(b)).

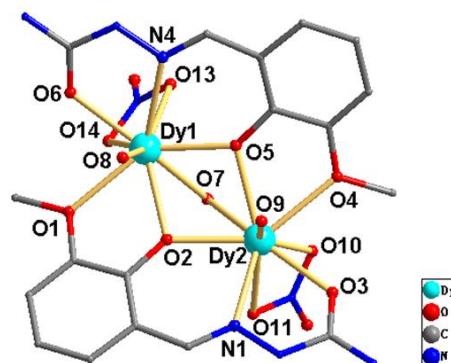


Figure 2. Molecular structures of coordination compound **3**. Hydrogen atoms and lattice solvent molecules are omitted for clarity.

Magnetic properties

In order to confirm the phase purity, the powder X-ray diffraction (PXRD) measurements for the bulk samples of coordination compounds **1-3** have been examined (Figure S3). These results were in good agreement with XRD patterns calculated from the single-crystal data, indicating high purity of the obtained samples. The differences in reflection intensity are due to the preferred orientations of the powder samples during the collection of the experimental data.

Direct-current (dc) magnetic susceptibilities of **1-3** have been collected in an applied magnetic field of 1000 Oe in the temperature range of 300-1.8 K (Figure 3). For all coordination compounds, the room temperature $\chi_M T$ values are 27.4, 22.8 and 27.6 for **1-3**, respectively, these are in reasonable agreement with two uncoupled Ln^{III} ions: two Dy^{III} ions ($^6H_{15/2}$, $S = 5/2$, $L = 5$, $g = 4/3$) give $28.34 \text{ cm}^3 \text{ K mol}^{-1}$ for **1** and **3**, two Er^{III} ($^4I_{15/2}$, $S = 3/2$, $L = 6$, $g = 6/5$) give $22.96 \text{ cm}^3 \text{ K mol}^{-1}$ for **2**. Upon cooling, the temperature dependence of the magnetic susceptibilities of three cases exhibit similar thermal evolution. As the temperature is lowered, $\chi_M T$ values steadily decrease from 300 to 50 K and then the curves rapidly decrease to a minimum of $5.08 \text{ cm}^3 \text{ K mol}^{-1}$ for **1**, $5.16 \text{ cm}^3 \text{ K mol}^{-1}$ for **2** and $20.22 \text{ cm}^3 \text{ K mol}^{-1}$ for **3**. This behavior could arise from the progressive depopulation of the Ln^{III} ions excited m_J sublevels and potential weak antiferromagnetic interactions between the Ln^{III} ions.

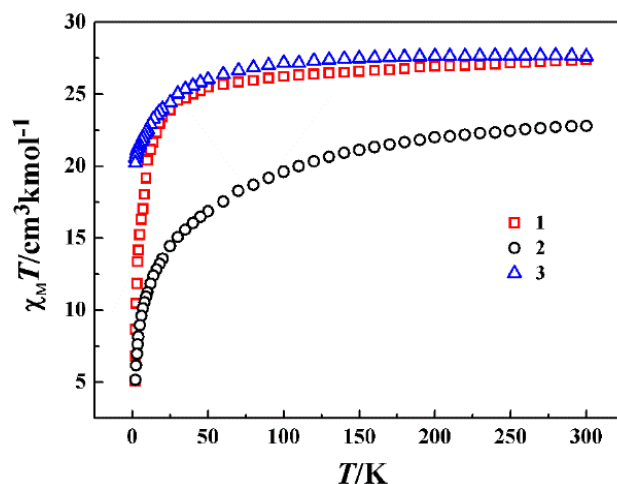


Figure 3. Temperature dependence of the $\chi_M T$ values for coordination compounds **1-3** in 1000 Oe.

The magnetization data of **1-3** were carried out at the 0-70 kOe field range below 5 K. The M vs. HT^{-1} data at 2.0–5.0 K show non-superimposed magnetization curves for coordination compound **1**, which suggests the presence of a significant anisotropy and/or low-lying excited states (Figure 4). Furthermore, the isothermal magnetizations of **2** and **3** show a rapid increase under low fields and then slowly increase in high fields without clear saturation through increasing dc field (Figure S4). The magnetization values of **1** (17.1 $N\beta$), **2** (11.2 $N\beta$) and **3** (14.4 $N\beta$) at 2K and 70 kOe are lower than the expected saturation value, which suggests there might be the ligand-field-induced splitting of the Stark level as well as significant magnetic anisotropy within the molecule.^[18]

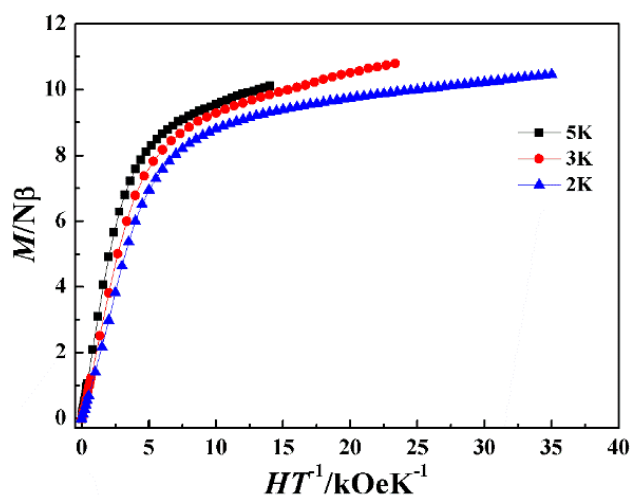


Figure 4. Field dependence of magnetizations of **1** at different temperatures below 5 K.

Alternating-current (ac) magnetic measurements were carried out under zero dc fields for **1-3**. No out-of-phase (χ''_M) signals were observed for **2** and **3** (Figure S5-S6), but well defined temperature-dependent χ''_M maximum at low temperatures was observed for **1** (Figure 5a), indicating the presence of slow magnetic relaxation at lower temperature, typical of SMM behavior. The clear peaks can be detected at frequencies higher than 100 Hz in χ'' vs. T plots, indicating that blocking is not complete and thermally activated spin reversal is gradually replaced by a quantum tunneling mechanism at zero dc field.^[19] The magnetization relaxation time (τ) has been estimated from the χ'' peaks using the Arrhenius law, $\tau = \tau_0 \exp(U_{\text{eff}}/k_B T)$ (Figure S7). The fitting results gave an anisotropic energy barrier $U_{\text{eff}} = 26.7\text{K}$ and the pre-exponential factors $\tau_0 = 1.68 \times 10^{-6}$ s for **1**, the τ_0 value is notably larger than the expected values of around 10^{-9} - 10^{-11} for a SMM.^[20]

For further understanding the magnetic behavior of **1**, variable-frequency ac susceptibility measurements have been conducted under zero dc field. Compound **1** revealed a χ'' component signal in 3K and 5K, but the maxima of the signals lie outside the accessible frequency range of the instrument (Figure S8). To observe maxima on the χ'' vs. ν plot for **1**, the ac measurements were conducted under an applied dc field of 1200 Oe. The frequency-dependent χ' and χ'' signals and maximum values in out-of-phase ac susceptibility are observed in the temperature range 2.0-5.0 K, which also reveals the presence of slow relaxation of magnetization in **1** (Figure 5b). The Cole–Cole diagrams (Figure 6) in the form of χ'' vs. χ' from 2.0 to 5.0 K for **1** show an ideal semi-circular shape and are fitted by the generalized Debye model,^[21] with α values below 0.18, which indicates a relatively narrow distribution of the relaxation processes.

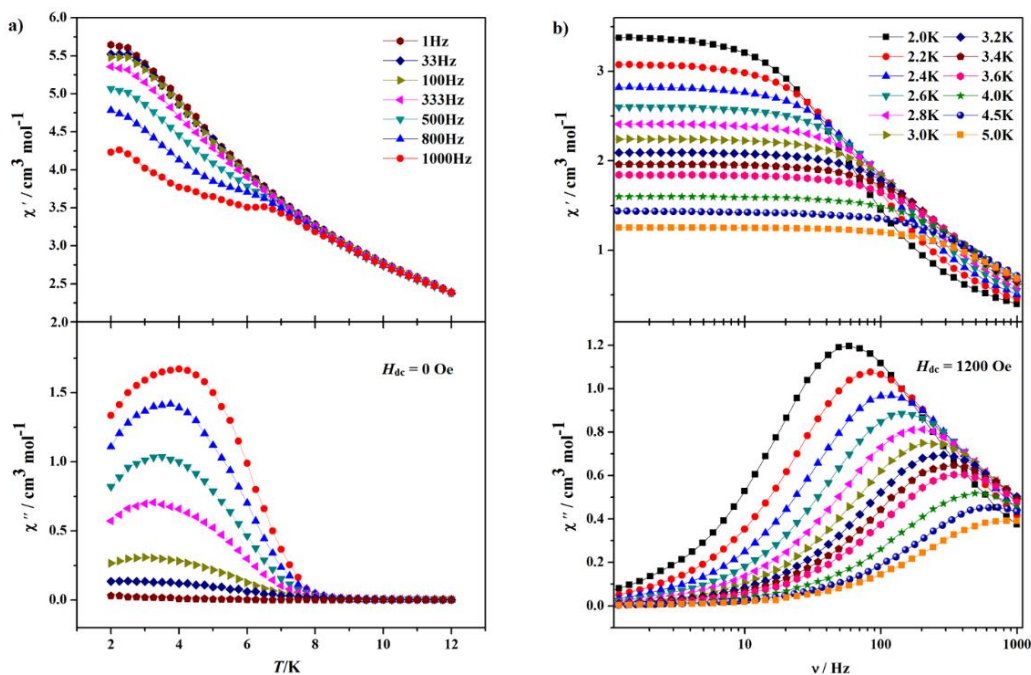


Figure 5. (a) Temperature-dependent in-phase χ' (top) and out-of-phase χ'' (bottom) ac susceptibility signals for **1** at the indicated frequencies under zero dc field; (b) frequency dependence of the in-phase χ' (top) and out-of phase χ'' (bottom) ac susceptibility signals for **1** under 1200 Oe dc field.

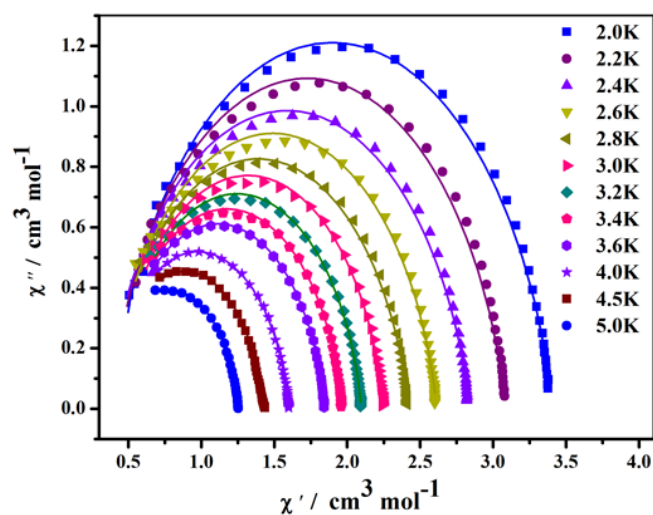


Figure 6. The Cole–Cole plots at 2.0–5.0 K of **1** under 1200 Oe. The solid lines correspond to the best fit obtained with the Debye functions.

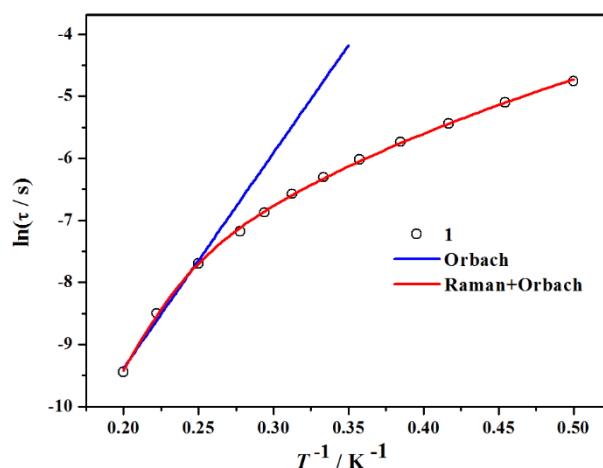


Figure 7. The plots of $\ln(\tau)$ vs. T^{-1} at the 1200 Oe dc field for **1**. The blue and red solid lines represent the fitting by the Arrhenius law for the high temperature region and for all the data, respectively.

The plots of $\ln(\tau)$ vs. T^{-1} in Figure 7 exhibit strong linear dependence of $\ln(\tau)$ at high temperatures which indicative of a dominant Orbach relaxation mechanism, while at lower temperatures $\ln(\tau)$ values progressively deviate from linear behavior below 4.0K, suggesting that thermally activated spin reversal is gradually replaced by multiple relaxation processes. As a temperature independent regime is not reached as well as an applied dc field of 1200 Oe, the quantum tunneling and direct processes are weak and can be neglected.^[22] Thereby the relaxation times (τ) is fitted by considering possible Raman and Orbach processes. The equation can be set by using:

$$\tau^{-1} = CT^n + \tau_0^{-1} \exp(-U_{\text{eff}}/k_B T) \quad (1)$$

It is evident from the equation (1) that Orbach process would take the main place at higher temperature when the temperature is much lower than the energy barrier. In case of **1**, at high temperature, if only use the Orbach process, the relaxation times (τ) extracted from the frequency-dependent data follow the Arrhenius law with the pre-exponential factor $\tau_0 = 4.15 \times 10^{-7}$ s and the effective barrier $U_{\text{eff}} = 28.77 \text{ cm}^{-1}$ (41.4 K). Furthermore, considering the Raman process, the points will be fitted with equation (1) in the whole temperature range. Fitting results give $C =$

$12.8 \text{ s}^{-1} \text{ K}^{-3.7}$, $n = 3.7$, $U_{\text{eff}} = 50.12 \text{ cm}^{-1}$ (72.1 K), $\tau_0 = 1.15 \times 10^{-8} \text{ s}$ for **1**. The results indicate that the magnetic relaxation occurs from the contributions of both Orbach and Raman processes for **1**.

Magneto-structural correlation

Magnetic analysis exhibits single-molecule magnet behavior of compound **1**. Actually, Lin group reported an extremely similar compound $[\text{Dy}_2(\text{Hhmc})_2(\text{NO}_3)_4] \cdot \text{THF} \cdot \text{MeCN}$ (**4**) ($\text{H}_2\text{hmc} = 1,5\text{-bis}(2\text{-hydroxy-3-methoxybenzylidene})\text{-carbonohydrazide}$) which shows non-SMM behavior, synthesized by symmetric double *o*-vanillin Schiff base ligand (Figure 8).^[12] Both **1** and **4** have the $[\text{Dy}_2(\text{L})_2(\text{NO}_3)_4]$ molecular structures wherein the Dy^{III} ions have the same coordination sphere, mainly differing on the size of ligand. The ligand used by compound **1** is only the effective coordination part of the ligand used by compound **4**. The geometry of **4** was also determined with the SHAPE 2.1 software, which reveal similar deviation from the capped square antiprismatic polyhedron with **1** (Table S3)^[17]. Meanwhile, it is undeniable that existing the difference of lattice solvent for **1** and **4** may affect the behavior of SMMs, but the weak intermolecular forces produced by solvent molecules not clearly affect the coordination configuration around Dy^{III} ions (Figure 8c), and the crystal system and space group of two compounds remain unchanged. Therefore, we think the difference of lattice solvent molecules in **1** and **4** is not the main factor of affecting the behavior of SMMs. In comparison with coordination environment of **1** and **4**, the bond distances of Dy-O/N in equatorial pentagonal plane in **1** uniformly shorter than those observed in **4** (Table 1), indicating that a relative strong transverse ligand field possibly exist in the local Dy^{III} sites of **1**.^[16] The phenomenon of the coordination bond length consistent change for pentagonal plane mainly caused by the difference of conjugated degree of two ligands. Single *o*-vanillin Hhms ligand shrinks the conjugate part 2-(hydrazonomethyl)-6-methoxyphenol (the part of blue dotted line in Figure 6b), which may in favor of weakening the electron-donating effect. Namely, strategically tailoring electron-donating part of ligand probably leads to transverse lower negative charge distributions around Dy^{III} ions which in favor of the occurrence of SMM behavior. Furthermore, the steric hindrance and electronic modifications in two ligand backbone provoke a slightly disparity of coordinated NO_3^- angles for **1** and **4**. The O5–Dy–O7 and O8–Dy–O9 angles for **4** are 50.77 (91°) and 52.72 (96°), while for **1** both angles are almost equal values 51.58 (11°) and 51.00 (10°), probably produce a relatively high axial symmetry for **1**, which is

likely to improve the relaxation performance of SMMs. Besides, the slight differences of Dy...Dy distances and Dy–O–Dy angles for coordination compounds **1** and **4** possibly have an influence on the magnetic exchange coupling between the two local Dy^{III} ions (Table 1). In sum, it can be commented that the different magnetic properties of **1** and **4** mainly result from the electronic modifications of two schiff base ligand backbone and rationally tailoring the electron-donating part on the ligand backbone probably in favor of the SMM behavior.

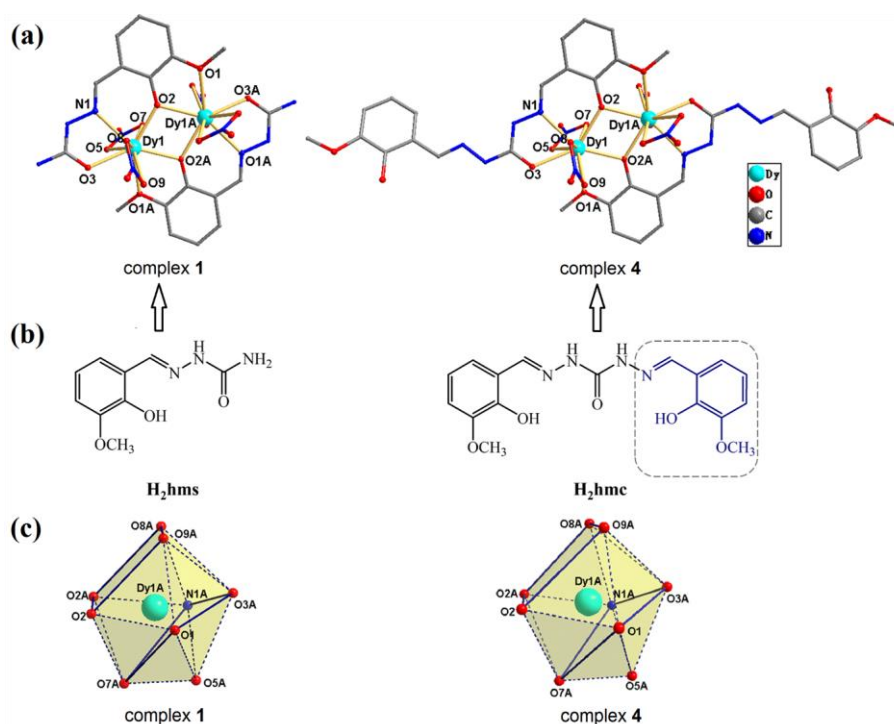


Figure 8. (a) Similar coordination environment of compound **1** and reported **4** in ref. 12; (b) The ligands used in compound **1** and reported **4** in ref. 12; (c) Coordination configuration around Dy centers observed in compound **1** and reported **4** in ref. 12.

Table 1. Some Selected Distances (Å) and Angles (deg) for Coordination Compound **1** and Reported **4** in Ref. 12.

	1	4
Dy1–O1A	2.405(3)	2.420(3)
Dy1–O2A	2.357(3)	2.367(3)
Dy1–O2	2.303(3)	2.313(3)
Dy1–O3	2.325(3)	2.343(3)
Dy1–N1	2.460(4)	2.465(3)
Dy1...Dy1A	3.6685(3)	3.7078(4)

Dy1-O2-Dy1A

103.885(11)

104.821(89)

In addition, the comparison of out-of-phase ac signal in compounds **1** and **3** reveals large discrepancy. Different from **1**, compound **3** does not show magnetic relaxation behavior. Though the coordination number of Dy^{III} centers not changed, the presence of one additional μ_2 -OH₂ bridge in **3** greatly influenced the Dy-O-Dy angles. The Dy^{III} ions in **1** are bridged by two μ -O bridge with the Dy-O-Dy angle of 103.87°, while in compound **3** with three μ -O bridge whose Dy-O-Dy angles vary from 89.83 to 101.68°, which are smaller than those observed in **1**. The change of the μ -O bridges seems adverse to persistent axially of Dy ions.^[23] Compound **1** has a local hula-hoop-like geometry, while additional μ_2 -OH₂ bridge induce the larger bent of geometrical configuration around Dy^{III} centers in **3**. Such destruction of hula-hoop-like geometry may have a great influence on the local tensor of anisotropy and their relative orientations on each Dy site. Actually, in previously reported a coordination compound Na[Dy₂(Hovph)₂(μ_2 -OH)(OH)(H₂O)₅]₃·Cl·3H₂O also exhibits a Dy₂(μ -O)₃ core, similar not exhibit any out-of-phase ac signal to that of **3**.^[16] Therefore, significant change of the μ -O bridge between the metal centers will modify the overlap between the magnetic orbitals of the Dy ions thus influence magnetic interactions for **1** and **3**.^[24] On the other hand, isomorphous compound **2** no characteristic slow magnetic relaxation was observed. This phenomenon has been illustrated by a recent review.^[3c, 25] The charge distribution of the ligand play an important role to control the magnetic anisotropy. Because of Ln^{III} ions in terms of “oblate” and “prolate” electron density distributions, a strong anisotropy can be achieved by using different direction ligand fields for the Dy^{III}-based and Er^{III}-based SMMs. Therefore, the H₂hms ligand failed to provide appropriate ligand field around Er^{III} ions for compound **2**.

Luminescence properties

The UV-vis absorption spectra of the free ligand H₂hms and compounds **1-3** were recorded in CH₃OH solution (10⁻⁵ mol L⁻¹) at room temperature (Figure 9). The main absorption peaks of the ligand have been observed at 238 nm, 300 nm and 369 nm, which could be attributed to the n → π^* and π → π^* electronic transitions of the ligand. The absorption profiles of **1-3** reveal analogous sets of absorption bands with slightly red shift (peak maxima around 255 nm, 306 nm and 378 nm)

compared to the free ligand. In the wavelength range of 338–450 nm, the broad low-energy absorption of compounds **1-3** indicate the influence of coordination effect between the ligand and the Ln^{III} cations.^[26]

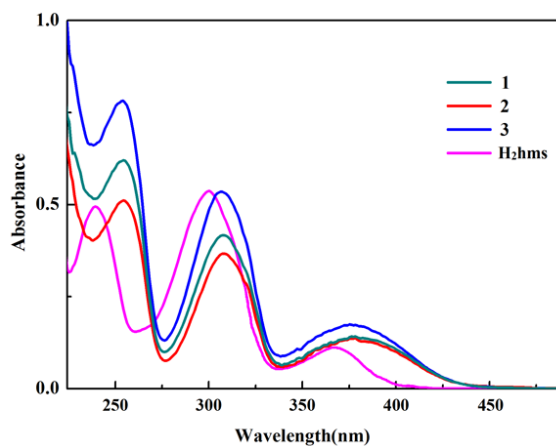


Figure 9. UV-vis absorption spectra of compounds **1-3** and the ligand (H₂hms) in CH₃OH solution at room temperature.

The luminescence spectra of coordination compounds **1-3** in the solid-state were measured. Efficient emission from the Dy³⁺ failed to be observed for compounds **1** and **3**, but the spectra show a ligand-centered emission (Figure S9).^[27] Optical excitation of compound **2** at 380 nm results in a typical emission signal in NIR region. The emission spectrum of **2** (Figure 10b) shows a single band at 1555 nm, which originates from the 4f-4f electronic transition of the first excited state (⁴I_{13/2}) to the ground state (⁴I_{15/2}) of the Er³⁺ ion.^[28] The excitation spectrum for compound **2** collected at an emission wavelength of 1555 nm, closely matched with the absorption of the ligand (Figure 10a). The phenomenon indicates ligand-to-metal energy-transfer process between the ligands and Er³⁺ ions.^[29]

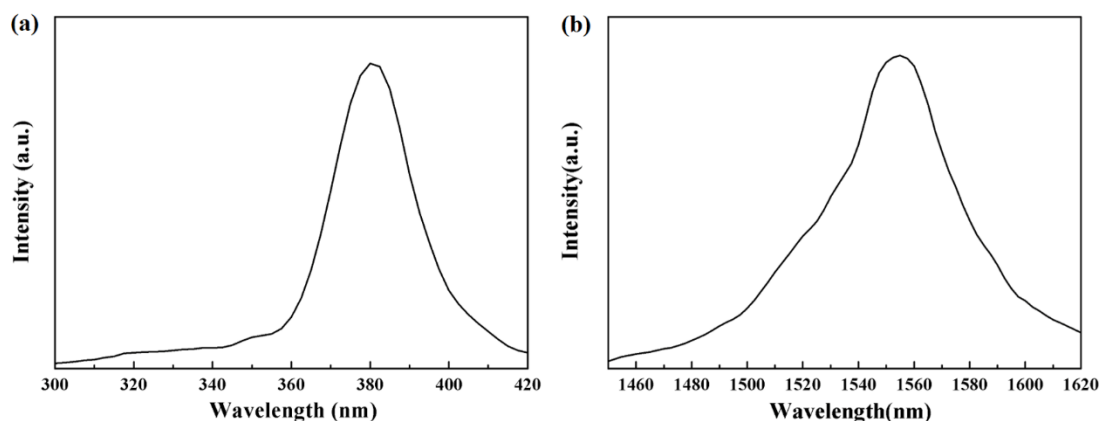


Figure 10. (a) The excitation spectrum of coordination compound **2** (λ_{em} = 1555 nm, black); (b) the room-temperature NIR emission spectra of coordination compound **2** (λ_{ex} = 380 nm) in the solid-state.

Conclusions

In summary, the structures, luminescent properties and magnetic properties of three dinuclear Ln^{III} coordination compounds based on tetradentate donor Schiff base ligand have been researched. The SMM/non-SMM behavior are further discussed based on two groups of Dy₂ compounds. Alternating-current magnetic susceptibility studies show that compound **1** exhibit frequency-dependent out-of-phase signals, while compound **3** and the Dy₂ compound in ref. 12 no ac signals are noticed. An additional μ_2 -OH₂ bridge in compound **3** broke the hula-hoop-like coordination geometry and induce smaller Dy-O-Dy angles, which may adverse to the SMM behavior. Compared with the Dy₂ compound in ref. 12, compound **1** exhibits extremely similar coordination environment. Maintaining the coordination configuration of the metal centers while changing conjugated degree of ligand backbone give rise to different magnetic properties. Fine-tuning of ligand field through changes of schiff base ligand backbone and μ -O bridges provides an elegant model to explore the influence of ligand filed effects on SMM properties in Dy₂ systems.

Experimental Section

Materials and methods

Commercially available reagents were used without further purification except for H₂hms was prepared according to the procedures reported previously. Elemental analysis for C, H and N were

carried out on a Elementar Vario EL III analyzer. The ^1H NMR spectra data were recorded using an AVANCE III Bruker 400 MHz instrument in a dimethyl sulfoxide (DMSO)- d_6 solution at room temperature. The FT-IR spectra were performed on KBr pellets on an EQUINOX 55 FT/IR spectrophotometer in the 400-4000 cm^{-1} region. The purity of the bulk samples was verified by powder X-ray diffraction (PXRD) measurements performed on a Bruker D8 ADVANCE X-ray powder diffractometer (Cu $K\alpha$, 1.5418 Å), with a scan speed of 5°min^{-1} and a step size of 0.04° in 2θ . UV-vis absorption studies were carried out with a Shimadzu UV-2450 spectrophotometer. Near-IR photophysical data were obtained on an Edinburgh FLSP920 fluorescence spectrometer. Magnetic susceptibility measurements were performed in the temperature range 2-300 K, using a Quantum Design MPMS XL-7 SQUID magnetometer equipped with a 7 T magnet. The experimental magnetic susceptibility data were corrected for the diamagnetism estimated from Pascal's tables and sample holder calibration. Alternating current (AC) susceptibility experiments were performed using an oscillating AC field of 3.5 Oe. The magnetization was measured in the field range 0-7 T.

Synthesis of (2-hydroxy-3-methoxybenzylidene)-semicarbazide (H_2hms)

The ligand was synthesized through a condensation reaction, following previously reported procedure.^[30] Semicarbazide hydrochloride and solid hydroxide were dissolved in distilled water and stirred for 30 min, a solution of o-vanillin in ethanol was added in a 1:1 ratio. After being refluxed and stirred at 80°C for 1h, the resulting yellow (or colorless) powder was collected through suction filtration and washed with a small amount of ethanol. IR (KBr pellet, cm^{-1}): 3425 (m), 3071 (m), 2653 (m), 2537 (m), 1930 (w), 1687 (s), 1593 (s), 1509 (m), 1421 (m), 1318 (s), 1278 (s), 1174 (s), 1113 (m), 1012 (w), 944 (w), 851 (m), 775 (m), 704 (w), 657 (w), 529 (w). ^1H NMR (DMSO- d_6): δ 10.22 (s, 1H), 9.29 (s, 1H), 8.17 (s, 1H), 7.39 (d, 1H), 6.92 (d, 1H), 6.77 (t, 1H), 6.42 (s, 2H), 3.81 (s, 3H) (Figure S10).

Preparation of the coordination compounds 1-3

Synthesis of $[\text{Dy}_2(\text{Hhms})_2(\text{NO}_3)_4]\cdot\text{MeCN}$ (1). To a solution of $\text{Dy}(\text{NO}_3)_3\cdot 6\text{H}_2\text{O}$ (0.4 mmol) and H_2hms (0.1 mmol) in methanol (10 mL) was dropwise added sodium azide (0.2 mmol). After stirring for 3 h, the resultant solution was filtered and allowed to stand undisturbed at room temperature. Block crystals suitable for single-crystal X-ray diffraction were obtained by slow evaporation of the filtrate after 1 month. Yield 48% based on Dy. Anal. Elemental analysis (%):

Calcd for $C_{22}H_{26}Dy_2N_{12}O_{18}$: H, 2.446; C, 24.661; N, 15.686. Found: H, 2.517; C, 25.310; N, 15.713. IR (KBr, cm^{-1}): 3347 (s), 3192 (s), 2418 (w), 1628 (s), 1511 (s), 1427 (s), 1280 (s), 1176 (m), 1083 (m), 968 (m), 891 (w), 783 (m), 739 (s), 583 (m), 438 (m), 406 (w).

Synthesis of $[Er_2(Hhms)_2(NO_3)_4] \cdot MeCN$ (2). Single crystals of **2** were obtained by a similar method as **1**. To a solution of $Er(NO_3)_3 \cdot 6H_2O$ (0.4 mmol) and H_2hms (0.1 mmol) in methanol (10 mL) was dropwise added sodium azide (0.2 mmol). After stirring for 3 h, the resultant solution was filtered and allowed to stand undisturbed at room temperature. Block crystals suitable for single-crystal X-ray diffraction were obtained by slow evaporation of the filtrate after 1 month. Yield 52% based on Er. Anal. Elemental analysis (%): Calcd for $C_{22}H_{26}Er_2N_{12}O_{18}$: H, 2.424; C, 24.444; N, 15.548. Found: H, 2.221; C, 23.462; N, 15.637. IR (KBr, cm^{-1}): 3340 (s), 2955 (m), 2426 (w), 1829 (w), 1627 (s), 1570 (s), 1423 (s), 1384 (s), 1280 (s), 1174 (m), 1100 (m), 964 (m), 826 (m), 759 (s), 568 (m), 426 (m), 408 (s).

Synthesis of $[Dy_2(Hhms)_2(NO_3)_2(H_2O)_3] \cdot (NO_3)_2 \cdot MeCN \cdot (H_2O)_2$ (3). To a solution of $Dy(NO_3)_3 \cdot 6H_2O$ (0.4 mmol) and H_2hms (0.1 mmol) in methanol (10 mL) was dropwise added triethylamine (0.2 mmol). After stirring for 3 h, the resultant solution was filtered and allowed to stand undisturbed at room temperature. Block crystals suitable for single-crystal X-ray diffraction were obtained by slow evaporation of the filtrate after 1 month. Yield 42% based on Dy. Anal. Elemental analysis (%): Calcd for $C_{20}H_{33}Dy_2N_{11}O_{23}$: H, 2.968; C, 21.438; N, 13.750. Found: H, 2.87; C, 21.010; N, 14.283. IR (KBr, cm^{-1}): 3408 (s), 2483 (w), 2343 (w), 1627 (s), 1589 (s), 1467 (s), 1328 (s), 1279 (s), 1173 (m), 1101 (m), 951 (m), 839 (m), 768 (m), 635 (m), 431 (m), 411 (w).

X-ray crystallography.

The single crystal X-ray experiment was performed on a Bruker Smart Apex II CCD diffractometer equipped with graphite monochromatized Mo $K\alpha$ radiation ($\lambda = 0.71073 \text{ \AA}$) using ω and ϕ scan modes at room temperature. The data integration and reduction were processed with SAINT software. Absorption corrections were applied using the SADABS program.^[31] The single-crystal structures were solved by direct methods using SHELXTL and refined by means of full-matrix least-squares procedures on F^2 using SHELXS-97 programs.^[32] All non-hydrogen atoms were located using subsequent Fourier-difference methods and refined anisotropically. The hydrogen atoms were placed in geometrically calculated positions. The crystal data and structure refinement details are summarized in Table 2. The selected bond lengths and angles are listed in

Table S4.

Table 2 Crystal data and structure refinement summary for coordination compounds **1-3**.

	1	2	3
Empirical formula	C ₂₂ H ₂₆ Dy ₂ N ₁₂ O ₁₈	C ₂₂ H ₂₆ Er ₂ N ₁₂ O ₁₈	C ₂₀ H ₃₃ Dy ₂ N ₁₁ O ₂₃
Formula weight	1071.55	1081.07	1120.57
Crystal system	triclinic	triclinic	monoclinic
Space group	$P\bar{1}$	$P\bar{1}$	$P2_1/c$
<i>a</i> (Å)	8.4653(8)	8.4989(15)	19.964(3)
<i>b</i> (Å)	10.0206(10)	9.9725(18)	7.8100(13)
<i>c</i> (Å)	10.7369(10)	10.724(2)	23.896(4)
α (°)	99.2780(10)	99.082(2)	90
β (°)	103.2150(10)	103.384(2)	97.894(3)
γ (°)	98.5190(10)	98.547(3)	90
<i>V</i> (Å ³)	858.69(14)	856.8(3)	3690.5(11)
<i>Z</i>	1	1	4
<i>D_c</i> (g m ⁻³)	2.072	2.095	2.017
μ (mm ⁻¹)	4.412	4.959	4.120
<i>F</i> (000)	518.0	522.0	2184.0
Reflns	4284	4212	19655
<i>R</i> _{int}	0.0138	0.0150	0.0552
Independent reflns	2976	2962	7819
GOF on <i>F</i> ²	1.016	1.046	0.985
<i>R</i> ₁ ^a [<i>I</i> > 2σ(<i>I</i>)]	0.0209	0.0265	0.0473
<i>wR</i> ₂ ^b (all data)	0.0777	0.0953	0.1243

^a $R_1 = \Sigma(|F_o| - |F_c|) / \Sigma|F_o|$, ^b $wR_2 = [\Sigma w(F_o^2 - F_c^2)^2 / \Sigma w(F_o^2)^2]^{1/2}$.

Supporting Information

Electronic Supplementary Information (ESI) available: selected bond lengths and bond angles, ¹H NMR spectra data of ligand, XRPD patterns and additional figures from the magnetic tests. CCDC 1483711-1483713. For ESI and crystallographic data in CIF or other electronic format see DOI:

Acknowledgements

We gratefully acknowledge financial support from the National Natural Science Foundation of China (grant nos. 21673180, 21373162, 21473135 and 21173168).

Keywords: Dinuclear compounds•Lanthanides•Magnetic properties•Schiff base ligand•Single-molecule magnets

References

- [1] a) P. Zhang, Y. N. Guo and J. K. Tang, *Coord. Chem. Rev.* **2013**, *257*, 1728-1763; b) L. Ungur, S. Y. Lin, J. K. Tang and L. F. Chibotaru, *Chem. Soc. Rev.* **2014**, *43*, 6894-6905; c) L. K. Thompson and L. N. Dawe, *Coord. Chem. Rev.* **2015**, *289-290*, 13-31; d) S. Demir, I.R. Jeon, J. R. Long and T. D. Harris, *Coord. Chem. Rev.* **2015**, *289-290*, 149-176; e) G. Aromi, D. Aguila, P. Gamez, F. Luis and O. Roubeau, *Chem. Soc. Rev.* **2012**, *41*, 537-546; f) D. N. Woodruff, R. E. Winpenny and R. A. Layfield, *Chem. Rev.* **2013**, *113*, 5110-5148; g) S. T. Liddle and J. van Slageren, *Chem. Soc. Rev.* **2015**, *44*, 6655-6669; h) L. Sorace, C. Benelli and D. Gatteschi, *Chem. Soc. Rev.* **2011**, *40*, 3092-3104; i) C. Benelli and D. Gatteschi, *Introduction to Molecular Magnetism: From Transition Metals to Lanthanides*, Wiley, **2015**; j) S. Gao, *Molecular nanomagnets and related phenomena*, Springer, **2015**.
- [2] a) F. Habib and M. Murugesu, *Chem. Soc. Rev.* **2013**, *42*, 3278-3288; b) S. Gómez-Coca, D. Aravena, R. Morales and E. Ruiz, *Coord. Chem. Rev.* **2015**, *289-290*, 379-392; c) P. Zhang, L. Zhang and J. K. Tang, *Dalton trans.* **2015**, *44*, 3923-3929.
- [3] a) J. Liu, Y. C. Chen, J. L. Liu, V. Vieru, L. Ungur, J. H. Jia, L. F. Chibotaru, Y. Lan, W. Wernsdorfer, S. Gao, X. M. Chen and M. L. Tong, *J. Am. Chem. Soc.* **2016**, *138*, 5441-5450; b) Y. C. Chen, J. L. Liu, L. Ungur, J. Liu, Q. W. Li, L. F. Wang, Z. P. Ni, L. F. Chibotaru, X. M. Chen and M. L. Tong, *J. Am. Chem. Soc.* **2016**, *138*, 2829-2837; c) W. B. Sun, P. F. Yan, S.D. Jiang, B. W. Wang, Y. Q. Zhang, H. F. Li, P. Chen, Z. M. Wang and S. Gao, *Chem. Sci.* **2016**, *7*, 684-691; d) Y. N. Guo, L. Ungur, G. E. Granroth, A. K. Powell, C. Wu, S. E. Nagler, J. K. Tang, L. F. Chibotaru and D. Cui, *Sci. rep.* **2014**, *4*, 5471.
- [4] a) R. J. Blagg, C. A. Muryn, E. J. McInnes, F. Tuna and R. E. Winpenny, *Angew. Chem. Int. Ed. Engl.* **2011**, *50*, 6530-6533; b) P. F. Yan, P. H. Lin, F. Habib, T. Aharen, M. Murugesu, Z. P. Deng, G. M. Li and W. B. Sun, *Inorg. Chem.* **2011**, *50*, 7059-7065; c) Y. N. Guo, X. H. Chen, S. Xue and J. K. Tang, *Inorg. Chem.* **2012**, *51*, 4035-4042; d) M. Yadav, A. Mondal, V. Mereacre, S. K. Jana, A. K. Powell and P. W. Roesky, *Inorg. Chem.* **2015**, *54*, 7846-7856.
- [5] a) S. Das, A. Dey, S. Kundu, S. Biswas, R. S. Narayanan, S. Titos-Padilla, G. Lorusso, M. Evangelisti, E. Colacio, V. Chandrasekhar, *Chem. Eur. J.* **2015**, *21*, 16955-16967; b) V. Chandrasekhar, S. Das, A. Dey, S. Hossain, J. P. Sutter, *Inorg. Chem.* **2013**, *52*, 11956-11965; c) S. Das, S. Hossain, A. Dey, S. Biswas, J. P. Sutter, V. Chandrasekhar, *Inorg. Chem.* **2014**, *53*, 5020-5028.
- [6] a) Y. N. Guo, G. F. Xu, W. Wernsdorfer, L. Ungur, Y. Guo, J. K. Tang, H. J. Zhang, L. F. Chibotaru and A. K. Powell, *J. Am. Chem. Soc.* **2011**, *133*, 11948-11951; b) W. Y. Zhang, Y. M. Tian, H. F. Li, P. Chen, W. B. Sun, Y. Q. Zhang and P. F. Yan, *Dalton trans.* **2016**, *45*, 3863-3873; c) J. Wu, L. Zhao, P. Zhang, L. Zhang, M. Guo and J. K. Tang, *Dalton trans.* **2015**, *44*, 11935-11942; d) C. Y. Chow, H. Bolvin, V. E. Campbell, R. Guillot, J. W. Kampf, W. Wernsdorfer, F. Gendron, J. Autschbach, V. L. Pecoraro, T. Mallah, *Chem. Sci.* **2015**, *6*, 4148-4159; e) X. Yi, K. Bernot, F. Pointillart, G. Poneti, G. Calvez, C. Daiguebonne, O. Guillou, R. Sessoli, *Chem. Eur. J.* **2012**, *18*, 11379-11387; f) W. H. Zhu, S. Li, C. Gao, X. Xiong, Y. Zhang, L. Liu, A. K. Powell, S. Gao, *Dalton trans.* **2016**, *45*, 4614-4621; g) Y. Peng, V. Mereacre, A. Baniodeh, Y. Lan, M. Schlageter, G. E. Kostakis, A. K. Powell, *Inorg. Chem.* **2016**, *55*, 68-74; h) X. Yi, G. Calvez, C. Daiguebonne, O. Guillou, K. Bernot, *Inorg. Chem.* **2015**, *54*, 5213-5219; i) J. Long, F. Habib, P. H. Lin, I. Korobkov, G. Enright, L. Ungur, W. Wernsdorfer, L. F. Chibotaru, M. Murugesu, *J. Am. Chem. Soc.* **2011**, *133*, 5319-5328.
- [7] F. Habib, G. Brunet, V. Vieru, I. Korobkov, L. F. Chibotaru and M. Murugesu, *J. Am. Chem. Soc.* **2013**, *135*, 13242-13245.
- [8] J. D. Rinehart, M. Fang, W. J. Evans and J. R. Long, *J. Am. Chem. Soc.* **2011**, *133*, 14236-14239.

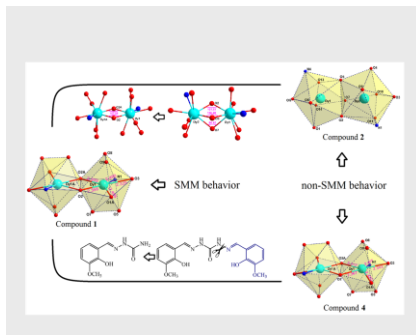
- [9] a) J. Wu, J. Jung, P. Zhang, H. Zhang, J. K. Tang, B. Le Guennic, *Chem. Sci.* **2016**, *7*, 3632-3639; b) P. Zhang, J. Jung, L. Zhang, J. K. Tang, B. Le Guennic, *Inorg. Chem.* **2016**, *55*, 1905-1911; c) X.L. Li, J. Wu, J. K. Tang, B. Le Guennic, W. Shi, P. Cheng, *Chem. Commun.* **2016**, *52*, 9570-9573; d) Y.N. Guo, G.-F. Xu, P. Gamez, L. Zhao, S.Y. Lin, R. Deng, J. K. Tang, H.J. Zhang, *J. Am. Chem. Soc.* **2010**, *132*, 8538-8539.
- [10] a) P. Bag, C. K. Rastogi, S. Biswas, S. Sivakumar, V. Mereacre, V. Chandrasekhar, *Dalton trans.* **2015**, *44*, 4328-4340; b) S. Biswas, S. Das, S. Hossain, A. K. Bar, J.-P. Sutter, V. Chandrasekhar, *Eur. J. Inorg. Chem.* **2016**, *28*, 4683-4692; c) S. Biswas, S. Das, G. Rogez, V. Chandrasekhar, *Eur. J. Inorg. Chem.* **2016**, *20*, 3322-3329; d) V. Chandrasekhar, S. Hossain, S. Das, S. Biswas, J. P. Sutter, *Inorg. Chem.* **2013**, *52*, 6346-6353.
- [11] A. J. Hutchings, F. Habib, R. J. Holmberg, I. Korobkov and M. Murugesu, *Inorg. Chem.* **2014**, *53*, 2102-2112.
- [12] C. J. Kuo, R. J. Holmberg and P. H. Lin, *Dalton trans.* **2015**, *44*, 19758-19762.
- [13] Y.L. Wang, C.B. Han, Y.Q. Zhang, Q.Y. Liu, C.-M. Liu and S.-G. Yin, *Inorg. Chem.* **2016**, *55*, 5578-5584.
- [14] W. M. Wang, H. X. Zhang, S. Y. Wang, H. Y. Shen, H. L. Gao, J. Z. Cui and B. Zhao, *Inorg. Chem.* **2015**, *54*, 10610-10622.
- [15] a) W. M. Wang, W. Z. Qiao, H. X. Zhang, S.Y. Wang, Y. Y. Nie, H. M. Chen, Z. Liu, H.-L. Gao, J.-Z. Cui and B. Zhao, *Dalton trans.* **2016**, *45*, 8182-8191; b) X. Zou, P. Yan, Y. Dong, F. Luan and G. Li, *RSC Adv.* **2015**, *5*, 96573-96579; c) V. Béreau, H. Bolvin, C. Duhayon, J.-P. Sutter, *Eur. J. Inorg. Chem.* **2016**, DOI: 10.1002/ejic.201600924.
- [16] Y. N. Guo, X. H. Chen, S. Xue and J. K. Tang, *Inorg. Chem.* **2011**, *50*, 9705-9713.
- [17] M. Llunell, D. Casanova, J. Cirera, J. M. Bofill, P. Alemany, S. Alvarez, SHAPE (version 2.1), Barcelona, **2013**.
- [18] a) S. Osa, T. Kido, N. Matsumoto, N. Re, A. Pochaba and J. Mrozinski, *J. Am. Chem. Soc.* **2004**, *126*, 420-421; b) J. K. Tang, I. Hewitt, N. T. Madhu, G. Chastanet, W. Wernsdorfer, C. E. Anson, C. Benelli, R. Sessoli and A. K. Powell, *Angew. Chem. Int. Ed. Engl.* **2006**, *45*, 1729-1733.
- [19] W.-M. Wang, S. Y. Wang, H. X. Zhang, H. Y. Shen, J. Y. Zou, H. L. Gao, J. Z. Cui, B. Zhao, *Inorg. Chem. Front.* **2016**, *3*, 133-141
- [20] a) Y. Gao, G. F. Xu, L. Zhao, J. K. Tang, Z. Liu, *Inorg. Chem.* **2009**, *48*, 11495-11497; b) F. Tuna, C. A. Smith, M. Bodensteiner, L. Ungur, L. F. Chibotaru, E. J. L. McInnes, R. E.P. Winpenny, D. Collison and R. A. Layfield, *Angew. Chem. Int. Ed.* **2012**, *51*, 6976; c) F. Pointillart, S. Klementieva, V. Kuropatov, Y. Le Gal, S. Golhen, O. Cador, V. Cherkasov and L. Ouahab, *Chem. Commun.* **2012**, *48*, 714.
- [21] D. Gatteschi, R. Sessoli, J. Villain, Molecular Nanomagnets, Oxford University Press, Oxford, **2006**.
- [22] a) M. Gregson, N. F. Chilton, A.M. Ariciu, F. Tuna, I. F. Crowe, W. Lewis, A. J. Blake, D. Collison, E. J. L. McInnes, R. E. P. Winpenny, S. T. Liddle, *Chem. Sci.* **2016**, *7*, 155-165; b) C. Gao, Q. Yang, B.W. Wang, Z.M. Wang, S. Gao, *CrystEngComm*, **2016**, *18*, 4165-4171; c) S. Titos-Padilla, J. Ruiz, J. M. Herrera, E. K. Brechin, W. Wernsdorfer, F. Lloret and E. Colacio, *Inorg. Chem.* **2013**, *52*, 9620.
- [23] P. Zhang, L. Zhang, S. Y. Lin, S. Xue and J. K. Tang, *Inorg. Chem.* **2013**, *52*, 4587-4592.
- [24] H. S. Ke, S. Zhang, X. Li, Q. Wei, G. Xie, W. Y. Wang and S. P. Chen, *Dalton trans.* **2015**, *44*, 21025-21031.
- [25] J. D. Rinehart and J. R. Long, *Chem. Sci.* **2011**, *2*, 2078.
- [26] H. L. Gao, L. Jiang, S. Liu, H. Y. Shen, W. M. Wang, J. Z. Cui, *Dalton trans.* **2016**, *45*, 253-264.

- [27] S.Y. Wang, W.M. Wang, H.X. Zhang, H.Y. Shen, L. Jiang, J.Z. Cui and H.L. Gao, *Dalton trans.* **2016**, *45*, 3362-3371.
- [28] a) M. Ren, Z. L. Xu, S. S. Bao, T. T. Wang, Z. H. Zheng, R. A. Ferreira, L. M. Zheng and L. D. Carlos, *Dalton trans.* **2016**, *45*, 2974-2982; b) P. Martin-Ramos, C. Coya, V. Lavin, I. R. Martin, M. R. Silva, P. S. Silva, M. Garcia-Velez, A. L. Alvarez and J. Martin-Gil, *Dalton trans.* **2014**, *43*, 18087-18096; c) W. Xu, Y. Zhou, D. Huang, W. Xiong, M. Su, K. Wang, S. Han and M. Hong, *Cryst. Growth Des.* **2013**, *13*, 5420-5432.
- [29] a) K. A. White, D. A. Chengelis, M. Zeller, S. J. Geib, J. Szakos, S. Petoud and N. L. Rosi, *Chem. Commun.* **2009**, 4506-4508; b) R. Fu, S. Hu and X. Wu, *Dalton trans.* **2009**, 9440-9445.
- [30] S. L. Li, D. X. Liu, J. H. Zhou and F. Q. Meng, *Chin. J. Struc. Chem.* **1995**, *14*, 88-93.
- [31] G. M. Sheldrick, *SADABS, Program for Empirical Absorption Correction, University of Göttingen, Göttingen, Germany, 1996*.
- [32] G. M. Sheldrick, *SHELXTL, Bruker Analytical X-ray Instruments, Inc., Madison, WI, 1998*.

Table of Contents

FULL PAPER

Magnetic studies of dinuclear Dy₂ compound [Dy₂(Hhms)₂(NO₃)₄]·MeCN have been performed and it shows slow relaxation of the magnetization at zero field and a thermal energy barrier $U_{\text{eff}} = 72.1$ K with $H_{\text{dc}} = 1200$ Oe. Compared with the other two analogous Dy₂ compounds, fine-tuning of ligand field is dominated by μ -O bridges and ligand backbone that cause the SMM/non-SMM behaviour.



Key Topic: Ligand field effect

Min Li, Haipeng Wu, Sheng Zhang, Lin Sun, Hongshan Ke, Qing Wei, Gang Xie, Sanping Chen*, Shengli Gao*

Page No. – Page No.

Fine-Tuning Ligand Field with Schiff Base Ligand in Dy₂ Compounds